Cost-effective PROton Exchange MEmbrane WaTer Electrolyser for Efficient and Sustainable Power-to-H2 Technology

Grant No. 862253

***Start date**: 01.04.2020 – **Duration**: 36 months*
***Project Coordinator**: Daniel García-Sánchez - DLR*

D1.4: Report on the final selection of electrocatalysts to be delivered for stacks' MEAs production

WP1 Catalyst Development

WP *Leader*: *CENmat*
Deliverable Responsible: *CNR*
Deliverable Author(s): Stefania Siracusano, Antonino Aricò (CNR); Sambal S Ambu, Seyed S Hosseiny (CENmat); María Retuerto, Sergio Rojas (CSIC); Meital Shviro (FZJ)

Status: F
(D: Draft, FD: Final Draft, F: Final)
Dissemination level: PU
(PU: Public, CO: Confidential,
only for Consortium members (including the Commission Services))

This project has received funding from the European Union's Horizon 2020 research and innovation programme under grant agreement No 862253

This project has received funding from the European Union's Horizon 2020 research and innovation programme under grant agreement No 862253.

Document history

Version Number	Date of issue	Author(s)	Brief description of changes
V 0	30/11/2021	Sambal S Ambu (CENmat)	Creation of CENmat report
V1	07/12/2021	Stefania Siracusano (CNR)	Creation of draft
V2	14/12/2021	Stefania Siracusano, Antonino Aricò (CNR)	Review and Redaction of 2st version

Table of Content

List of Figures

List of Tables

Acronyms

BET - Brunauer Emmett-Teller
CRM – Critical raw material
CV - Cyclic Voltammetry
ECSA- Electro chemical surface area
EDX- Energy-dispersive X-ray
EIS- Electrochemical Impedance Spectroscopy
HER- Hydrogen Evolution Reaction
ICP- Inductively Coupled Plasma
OER- Oxygen Evolution Reaction
OCP- Open circuit potential
MEA- Membrane electrode assembly
PEM- Proton Exchange Membrane
PEMWE- Proton exchange membrane water electrolysis
RDE -Rotating Disk Electrode
RHE- Reversible Hydrogen Electrode
SEM- Scanning Electron Microscopy
TEM -Transition Electron Microscopy
XPS- X-ray Photoelectron Spectroscopy
XRD- X-ray Diffraction
XRF – X-Ray fluorescence spectroscopy
WE - Working Electrode

1 Introduction

Deliverable D1.4 is a development report on the synthesis and performance of the final selection of catalysts for stack' MEA (Membrane Electrode Assembly) production.

Both CRM (critical raw material) reduced, and CRM free catalysts were prepared in appropriate amount for preparing MEAs and delivered to respective partner for single cell testing.

On the front of CRM reduced catalyst, a double perovskite with formula Sr_2MIrO_6 (M= Ca, Mg and Zn) is prepared by partner CSIC as OER catalyst. Partner CENmat has synthesized supported noble metal catalyst Ir@ATO and Pt@Mo_2C as OER and HER catalysts, respectively.

Along with the CRM reduced catalysts, Ag metallic electrocatalyst and Ag dispersed on Ti-suboxides catalyst is prepared by partner CNR as CRM free catalyst for OER and CSIC developed a MoS_2 supported on carbon black pearls (BP) CRM free catalyst for HER.

2 CRM reduced catalysts

2.1 Oxygen Evolution reaction (OER): *Ir@ATO*

CENmat (Cutting Edge nanomaterials) has taken the approach of finely dispersing the Ir nanoparticles on a support to increase the mass activity or Iridium, in turn reducing the amount of the Ir needed for PEMWE. Support material chosen for this purpose is antimony doped tin oxide (Sb-SnO_2) (ATO).

2.1.1 Synthesis and characterization

All the synthesis routes chosen are wet chemical synthesis routes for the ease of scalability. Two major synthesis routed takes were direct reduction of Ir salt precursor on ATO nanoparticles and deposition of Ir nano colloidal solution on ATO nano particles via stirring. Both the synthesis processes are discussed in brief to give a clear understanding.

In direct reduction synthesis ATO nano powder was dispersed in an organic solvent ethanol with the help of 15 mins of ultrasonication. A surfactant was dissolved in previously chosen organic solvent. In the next step above stated dispersion and solution were mixed in a 3 necked round bottom flask under inert atmosphere with the help of overhead stirrer or 30 min. Iridium precursor was then dissolved in the solvent and introduced into the above mixture and stirred for 3 h in inert atmosphere. After 3 hours a reducing agent solution was introduced into the above mixture. After the introduction of reducing agent, the mixture was left to stir for 4h. The mixture was left to sediment overnight. The supernatant was removed, and the synthesized catalyst was thoroughly washed with ethanol and water and collected with the help of centrifuge. After that the catalyst was dried overnight in a drying over at 50℃. The yield of the process was found to be 85%. This synthesis process in simple and inexpensive.
The target loading of the Ir on ATO particles in the described synthesis route were 10, 35 and 50 Wt.%.

In deposition synthesis route, $IrCl_3.xH_2O$ (Alfa Aesar) was weighted and dissolved in Ethylene glycol vis sonication. In the next step more EG was added to the above solution and is degassed with argon for one hour. In the next step the solution is heated in argon atmosphere at 145 °C for five hours and left to cool down overnight. As prepared Ir nanoparticles colloidal solution is very stable and does not precipitate ever after months. Going further ATO nano powder was dispersed in EG and sonicated for 30 mins. Ir colloidal solution was introduced into the ATO dispersion during sonication. After that the mixture was left to stir for 70 h. Ir coated ATO nanoparticles were then thoroughly washed with UP water and ethanol and dried in over overnight at 50 °C. The yield of the process is found to be 50%. The target loading of the Ir on ATO particles in the described synthesis route was 10, 35 and 50 Wt.%.

Apart from the above-mentioned catalysts many different catalysts are prepared including the risk mitigation catalyst called Ir nano. The catalyst prepared through deposition route has low yield and the controlling the Ir loading on ATO seemed to be difficult, so this synthesis route has not been explored more.

Ir@ATO (35 Wt.%) prepared through reduction was thoroughly characterized for surface morphology and elemental composition to understand how the Ir is dispersed on ATO nanoparticle and the difference between target and achieved Ir loading on ATO.

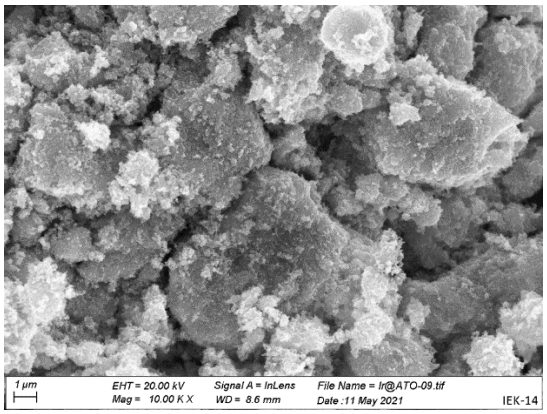

(a)

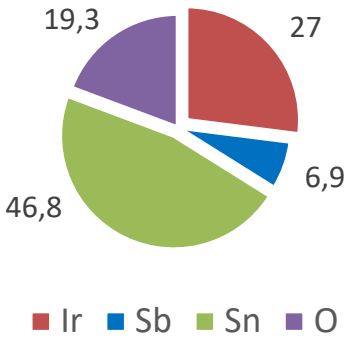

(b)

Figure 2. (a) SEM image and (b) elemental composition of newly developed Ir@ATO - Reduction (35 Wt.%) catalyst

From the SEM image (figure 1a) we can see the microscopic morphological features of the newly developed catalyst. The Ir dispersion on ATO looks to be in small nano agglomerate form resulting in the less catalyst surface area. The elemental composition of the catalyst is determined through EDX analysis.

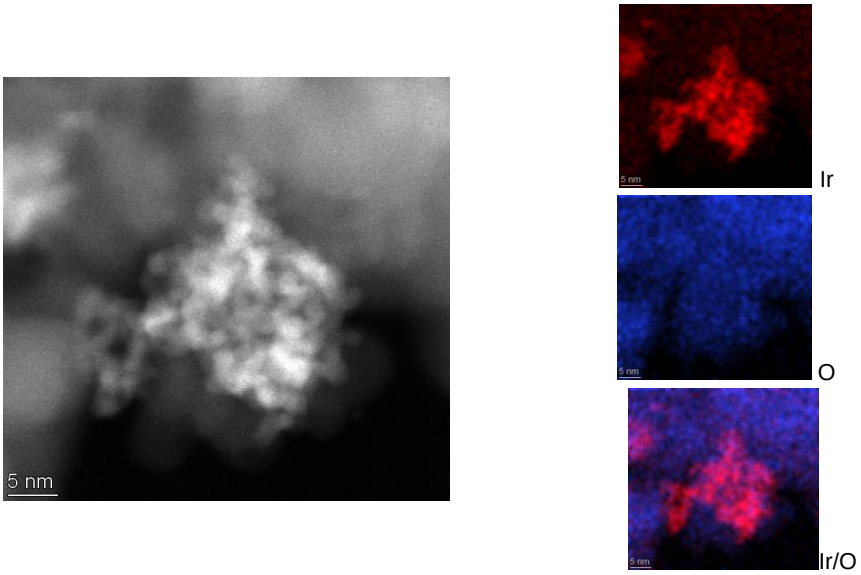

Figure 3. Elemental mapping of the Ir@ATO - Reduction (35 Wt.%)

As depicted in the (figure 1b) the average Ir content or loading on ATO is found to be 27 Wt.%. This loading is less than the intended Ir loading of 35 Wt.%, meaning the precursor amounts have to be tweaked to get to the desired Ir loading of 35 Wt.%.
Figure 2 shows the elemental mapping of the prepared catalyst. In this it is evident that the Ir is agglomerated on ATO particles and not perfectly homogenously dispersed.
To understand better the active area available in the prepared catalyst for the catalysis BET surface area was evaluated (figure 3). As we can see that even after visible agglomeration of Ir on ATO nanoparticles, developed catalyst has better surface area than the commercial IrO_2.

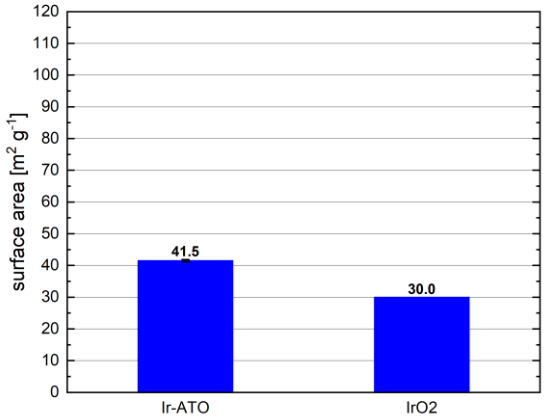

Figure 4. BET surface area of Ir@ATO - Reduction (35 Wt.%) and IrO_2

2.1.2 Electrochemical characterization

Electrochemical measurements (cyclic voltammetry ;CV) and linear polarization were performed in a three-electrode electrochemical cell. A reversible hydrogen electrode (RHE) and a high surface area platinum wire were used as reference and counter electrodes, respectively. A rotating disk electrode (RDE) with a 4 mm diameter glassy carbon electrode was used as working electrode. All potentials in this article are given with respect to RHE and all the experiments are done at ambient temperature and pressure. Catalytic inks were prepared by adding ultrapure water and isopropanol (3:1) (v/v) and nafion ionomer as binding agents to the dry catalyst (Ir@ATO) to obtain the desired suspension concentration. Ionomer to catalyst ratio was kept 0.2. The catalyst suspension was sonicated for 20 min in a sonication bath to achieve a homogeneous dispersion. The temperature of the bath was maintained at lower than 35 °C to avoid evaporation of solvent and agglomeration of the catalyst NPs. Prior to every measurement, the Glassy carbon working electrode (0.1256 cm^{-2}) was polished with 0.3 µm and 0.05 µm Al_2O_3 polishing suspension (Buhler AG) and thoroughly washed with ultrapure water.
0.5M electrolyte solutions were prepared from diluting down 2.5M H_2SO_4 (VWR) with ultrapure water (>18.2 MΩ). Electrochemical measurements were performed using an Gamary potentiostat. Afterward, the electrode was removed, dried, and coated with the catalyst ink by drop-casting and finally dried under a low argon flow over inverted RDE shaft at 400-600 rpm to have a homogeneous

catalyst layer. The total catalyst loading varied between 17-33 µg cm^{-2}. Electrolyte was bubbled with Ar gas before the start of the measurement for 20 mins.

Electrochemical measurement protocol consists of three sequences, a cyclic voltammetry within the voltage range 0.05-1.45 V, with a sweep rate 50 mV s^{-1} for three cycles to eradicate the influence of oxidation of impurities in oxidation current. In sequence LSVs were performed for three cycles within the voltage range 0.7-1.7 V with scan rate of 10 mV s^{-1}. The speed of rotation was 2500 rpm. All the results shown are iR corrected.

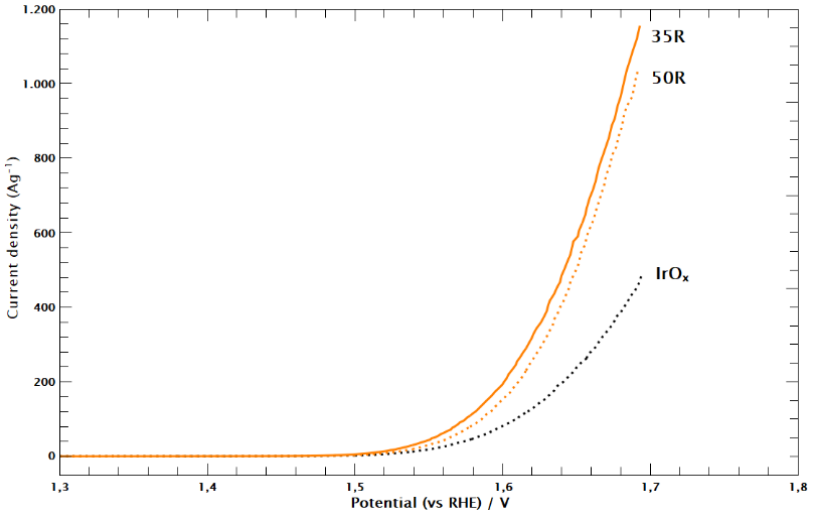

Figure 5. Area specific OER activity comparison on Ir O_x and newly developed catalyst

Figure 4 shows mass normalised LSV curve for the OER catalysts. In the figure above number (35 & 50) represent the intended loading of the catalyst on ATO nanoparticles. R represents reduction synthesis route. As shown in figure the mass specific OER activity of the synthesized catalysts were found to be better than that of IrO_x. These results show that the amount of noble metal can be reduced without affecting the OER activity.
Single cell testing is going on at CENmat and FZJ to analyze the stability of as synthesized catalyst.

Ir@ATO - Reduction (35 and 50 Wt.%) was tested in single cell by FZJ. As we can see in the figure 5, we can see the polarization curve of Ir@ATO - Reduction (50 Wt.%) and commercial IrO_x that at loading of 0.2 mg_{Ir} cm^{-2} and 2 mg_{Ir} cm^{-2} respectively. As we can see that even after reducing the catalyst loading 10 times the electrolyser performance remains approximately the same. Novel synthesized catalyst reaches 2.22 Acm^{-2} current density at 1.9 V with 0.2 mg_{Ir} cm^{-2} which surpasses the project target of 2 Acm^{-2} current density at 0.25 mg_{Ir} cm^{-2} loading.

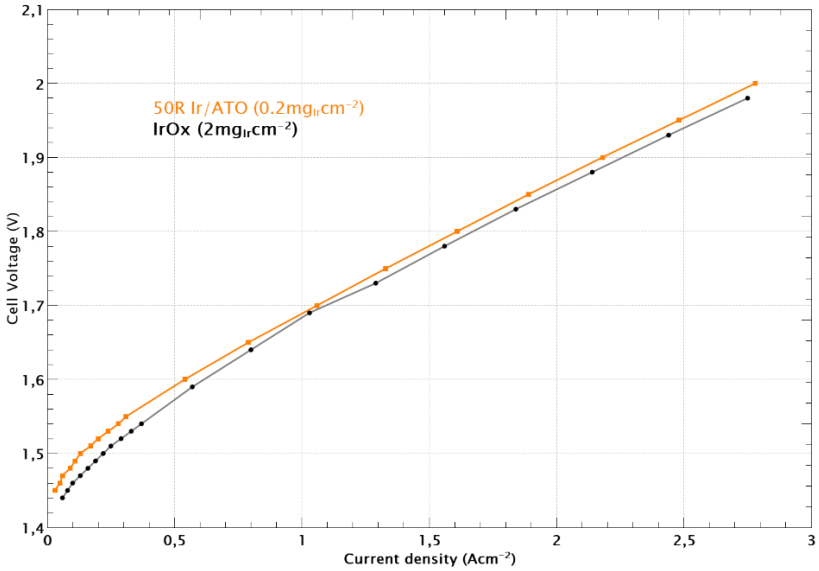

Figure 6. Polarization curve Ir@ATO - Reduction (50 Wt.%) and IrO_x

Stability of the catalyst at low loading is of utmost concern. FZJ has performed the stability study of novel synthesized catalyst Ir@ATO – Reduction (50 Wt.%) for 500 h at constant 2V. As we can see in the figure 6 that the current density at 2V of the single cell electrolyser has rather increased instead of decreasing, which indicated a good stability of the synthesized catalyst.

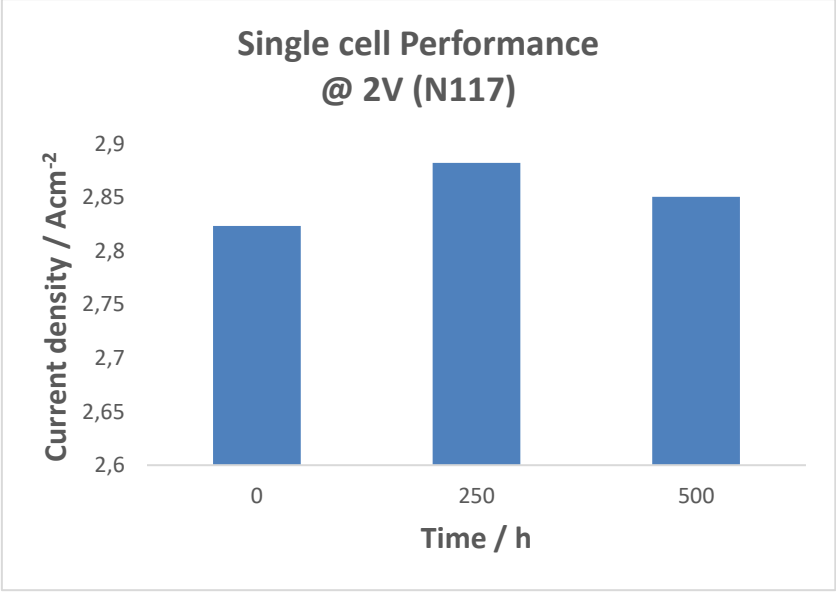

Figure 7. Current density of single cell electrolyser with Ir@ATO (50 wt.%) with 0.2 mg$_{Ir}$cm^{-2} for 500h

Since upscaling of the catalyst is a crucial part of the catalyst development, we have carefully chosen the synthesis routes to be simple and easily reproducible from the beginning. Most promising developed catalysts (Ir@ATO – Reduction) are prepared in bathes of 5-6 g of and have the potential to be up-scaled to be 15 grams catalyst per batch in our lab without any change in the material property.

2.2 Oxygen Evolution reaction (OER): *Sr_2CaIrO_6 and Y_2MnRuO_7*

Partner *CSIC* has taken the approach of preparing mixed oxides with reduced content of Ir and Ru. By this method it is possible to reduce the loading of the Ir needed for PEMWE. *CSIC* has chosen two mixed oxides to be tested in PEMWE:

Sr_2CaIrO_6

By designing this catalyst *CSIC* is reducing the content of Ir from state-of-the-art Ir catalysts. This oxide has been never tested for the OER, and *CSIC* has proven very high activity, and durability, related to the formation of a very active surface, rich o Ir.

Y_2MnRuO_7

By designing this catalyst *CSIC* is reducing the content of Ru in ruthenium pyrochlores without compromising the catalytic activity. *CSIC* was able to reduce Ru content in $Y_2Ru_2O_7$ by replacing half of Ru cations by Mn. Y_2RuMnO_7 has been never tested in acid media, and *CSIC* has proven a very high activity, stability and durability.

2.2.1 Synthesis and physicochemical characterization

Synthesis

Sr_2CaIrO_6 and **Y_2MnRuO_7**

Both mixed oxides have been prepared by the Pechini method. After the preparation of the precursors both samples were treated at high temperature in high pressure of oxygen to obtain the final catalysts.

Crystallographic Structures

Sr_2CaIrO_6 and **Y_2MnRuO_7**

Figure 7 shows the Rietveld refinement of the crystal structures of Sr_2CaIrO_6 (double perovskite) and Y_2MnRuO_7 (pyrochlore) using XRD data. Also, the TEM images are shown, in which the particle size, morphology, and structure are observed. The inset of the Figure depicts the schematic view of their crystal structures.

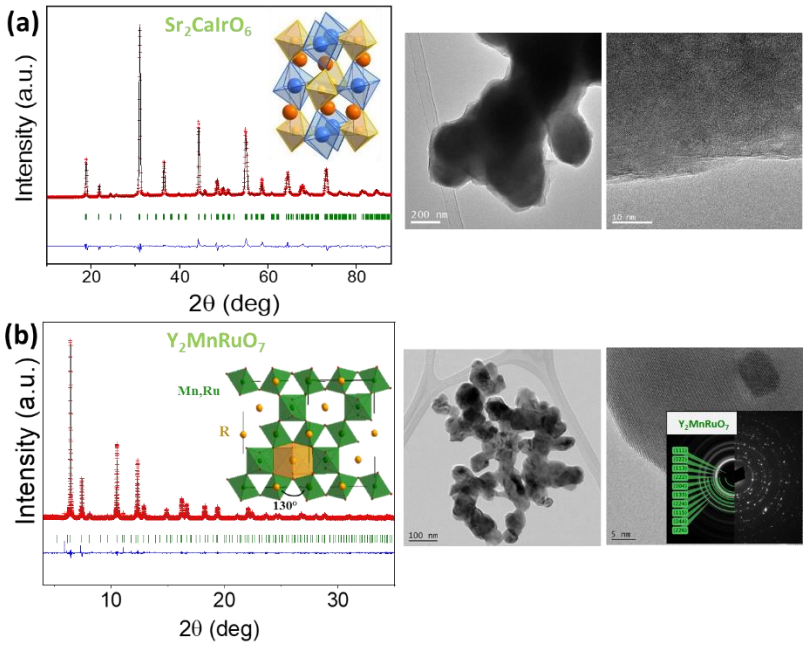

Figure 7. XRD and TEM of (a) Sr_2CaIrO_6 and (b) Y_2MnRuO_7 catalysts

2.2.2 Electrochemical Characterization Study: *Catalytic Performance*

OER Activity

The OER catalytic activity was measured in 0.1 M $HClO_4$ by cyclic voltammetry (CV) between 1.2 and 1.7 V vs. RHE, at 10 and 50 mV/s. Several measurements with different batches of catalysts have been performed to assess the reproducibility of the measurements.

Sr_2CaIrO_6

Sr_2CaIrO_6 catalyst presents very high OER activity (Figure 8a), especially by considering that the actual amount of Ir on the electrode is very low. For instance, Sr_2CaIrO_6 (ca. 4 $\mu g_{Ir}/cm^2_{electrode}$) achieves similar OER performance than IrO_x-Ir (10.2 $\mu g_{Ir}/cm^2_{electrode}$), which is one of the best OER catalyst reported till date.[1] The mass activity obtained for the catalyst is 97 A/g @ 1.48 V, higher than that of benchmark Ir catalysts. In the inset of Figure 2c the production of O_2 bubbles during the reaction is clearly observed, starting around 1.4 V, which is a very low overpotential for Ir-based catalysts.

Y_2MnRuO_7

Figure 8b shows the initial current density (*i*R corrected) obtained for Y_2MnRuO_7. The potential needed to attain 10 mA cm^{-2} is of only 1.50 V, which is lower than that reported for other Ru pyrochlores with higher content of Ru. [2]

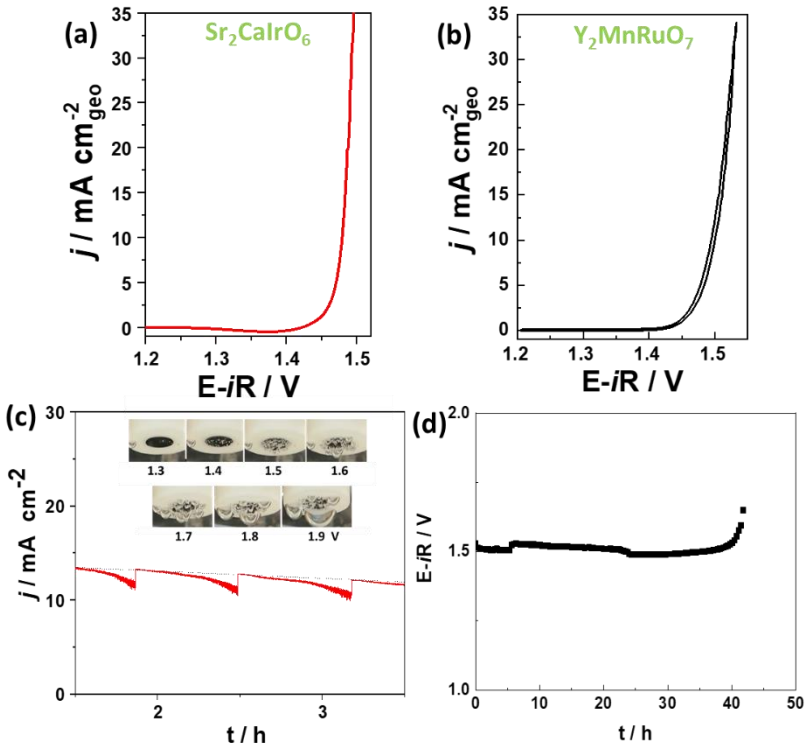

Figure 8. Polarization curves for (a) Sr_2CaIrO_6 and (b) Y_2MnRuO_7 in 0.1 M $HClO_4$ at 10 mV/s (c) Chronoamperometry of Sr_2CaIrO_6 during 4 hours at the potential where the current density is ca. 10 mA cm^{-2}. (d) Chronopotentiometry of Y_2MnRuO_7 during 40 hours at the current density where the potential is 1.5 V.

OER Durability

Several experiments have been performed to evaluate the stability of the catalysts. Consecutive OER cycles, chronoamperometry and chronopotentiometry measurements. Both catalysts are stable during tests (Figures 8c and 8d). It was only observed a loss of activity on Y_2MnRuO_7 after 40 hours at a constant current density where the potential was stable at 1.5 V for such time.

2.2.3 Post-mortem characterization

Both catalysts have been characterized after 2000 cycles of OER reaction. As shown in Figure 9, the evolution of both catalysts with the OER is very different.

On the one hand, Sr_2CaIrO_6, evolves during the reaction forming very open and active surface phases rich in Ir. (See TEM, XAS and XAS results in Figure 9a). The phases formed are mainly IrOOH phases with very active porous areas and holes.

On the other hand, the structure of Y_2MnRuO_7 remains unaltered during the catalytic testing with no visible changes in the morphology and composition of the cycled samples, indicating that the pyrochlore is stable, at least during 40 hours at high current densities.

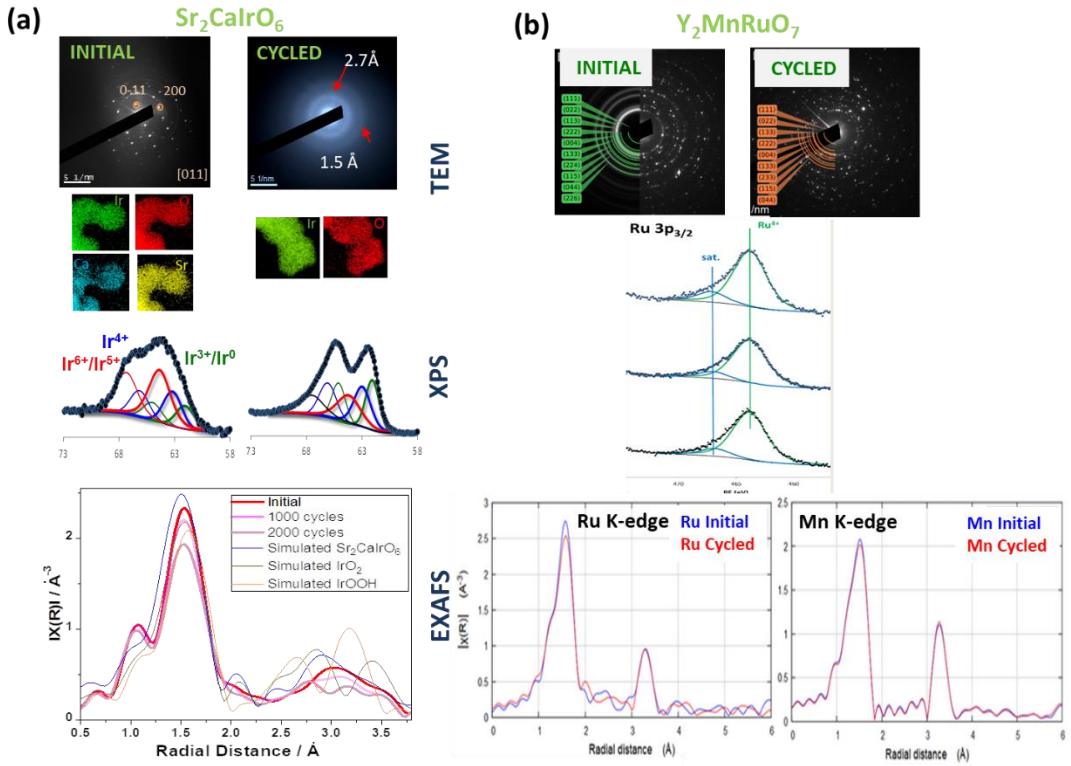

Figure 9. Post-mortem study of (a) Sr_2CaIrO_6 and (b) Y_2MnRuO_7. TEM images before and after OER cycles; XPS analysis before and after OER cycles; and EXAFS results before and after OER cycles

2.2.4 MEA Characterization

Sr_2CaIrO_6 and Y_2MnRuO_7 were sent to DLR to be tested in MEA. Preliminary results on PEMWE using Sr_2CaIrO_6 as the catalyst for the anode side have been already performed. Currently, measurements of the stability and the Ir loading on the MEAs are being performed. Figure 10 shows the E_{Cell}/j-characteristic up to 6 Acm^{-2} of the PEMWE cell using a MEA with Sr_2CaIrO_6 as anode catalyst. The curve reveals a performance of 2.4 V at peak current density showing a totally linear slope and with this not indicating any mass transport limitation. Comparing the cell performance of 2.09 V at 4 Acm^{-2} with the highest performances reported by other authors from prominent R&D institutes in electrolysis up to now the new catalyst is able to compete. [3–6] Furthermore, looking at the performance of commercial PEMWE from manufacturers such as Siemens, [7] Proton Onsite [8] and Hydrogenics [9], which achieve a potential of 2.2 V at 2 Acm^{-2}, however, a current of 4.8 Acm^{-2} can be achieved with the newly developed catalyst Sr_2CaIrO_6 at the same potential in comparison. Additionally, the EIS shown in the inset of Figure 5 explains the observed phenomena deeply. The Nyquist plots of the PEMWE cell with Sr_2CaIrO_6 as anode catalyst at 0.25, 1 and 4 Acm^{-2} are plotted. As described in previous work, an equivalent circuit was used as a basis to analyze the Nyquist spectra.[10] In short, while the intersection of the first semicircle in the high-frequency range with the x-axis can be determined as ohmic resistance, literature assign the high-frequency arc to different phenomena. On the one hand it can be related to the hydrogen evolution reaction (HER)[11], the charge transfer resistance coupled with double layer effects [9] or the first charge transfer of the two-electron process of the oxygen evolution reaction (OER) [12]. The charge transfer of the OER rate

determination step and the mass transport losses can be attributed to the medium and low frequency semicircle, respectively [13].

The Nyquist plot at 0.25 Acm^{-2} demonstrates one semicircle with a peak at a frequency of 54.99 Hz and is therefore mainly caused by charge transfer resistances with respect to OER. The interception with the x-axis account to an ohmic resistance of 118.4 $m\Omega cm^2$. Increasing the current density to 1 and 2 Acm^{-2} possible mass transport effects become more superficial. Both curves reveal again one semicircle which express the limitation by the OER kinetics as well as an ohmic resistance of 116.97 $m\Omega cm^2$ can be observed. This neglectable reduction in ohmic resistance of 1.43 $m\Omega cm^2$ compared to the Nyquist spectra at 0.25 Acm^{-2} can be explained by local heat generation at the interface of the MPL and CL at higher current densities.

Finally, no mass transport limitation can be observed neither in the polarization curve by for instance upwards bending of the curve[10], nor from the EIS since no semicircles in the low frequency range occur. Therefore, the recorded electrochemical data is in good agreement to each other.

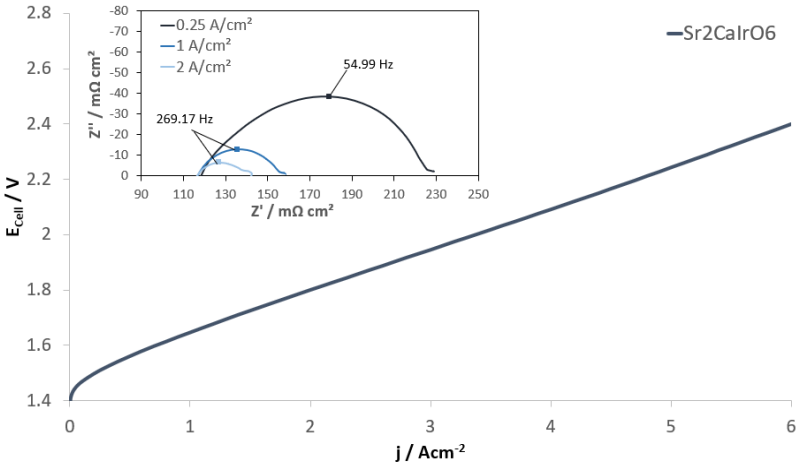

Figure 10. Polarization curve of Sr_2CaIrO_6 in PEMWE cell at 80 °C and atm. pressure up to 6 Acm^{-2}. The inset shows the Nyquist plots carried out at 0.25, 1 and 2 Acm^{-2} with an amplitude of 100, 500 and 1000 mA, respectively, from 100 mHz to 50 kHz.

2.3 Hydrogen Evolution Reaction (HER)

Partner *CSIC* is working on several catalysts for the HER with lower content of CRM. However, there are still not selected candidates to measure in MEAs since following studies have to be performed. *CSIC* is working in metallic phosphides, with different transition metals. Several phosphides are very promising for the HER, and some will be soon selected to be measured on MEA.

Partner *CENmat* has prepared a very low loading Pt@Mo_2C (5 wt.%) catalyst for facilitating hydrogen evolution reaction. The catalyst was prepared via a wet chemical synthesis route for the ease of scalability in the later stages of the project.

2.3.1 Synthesis and characterization

In brief 5.72 g of Mo_2C nano powder (commercial catalyst by CENmat) was dispersed in H_2O (>18.2 MΩ) with the help of ultrasonication. required amount of Pt precursor was then dissolved in water (>18.2 MΩ) via sonication of 15 mins and introduced into the above mixture in a three necked round bottom flask and stirred for 1 h. After 1 hours a reducing agent was dissolved in DI water and introduced into the above mixture. After the introduction of reducing agent, the mixture was left to stir for 70h. The mixture was left to sediment overnight. The supernatant was removed, and the synthesized catalyst was thoroughly washed with water and collected with the help of centrifuge. After that the catalyst was dried overnight in a drying oven at 50℃. The yield of the process was found to be 55%. Another risk mitigation catalyst Pt/C (5 wt.%) was synthesized the same way.
Developed catalyst were characterized for understand the morphology, composition surface area and dispersion of Pt on Mo_2C.

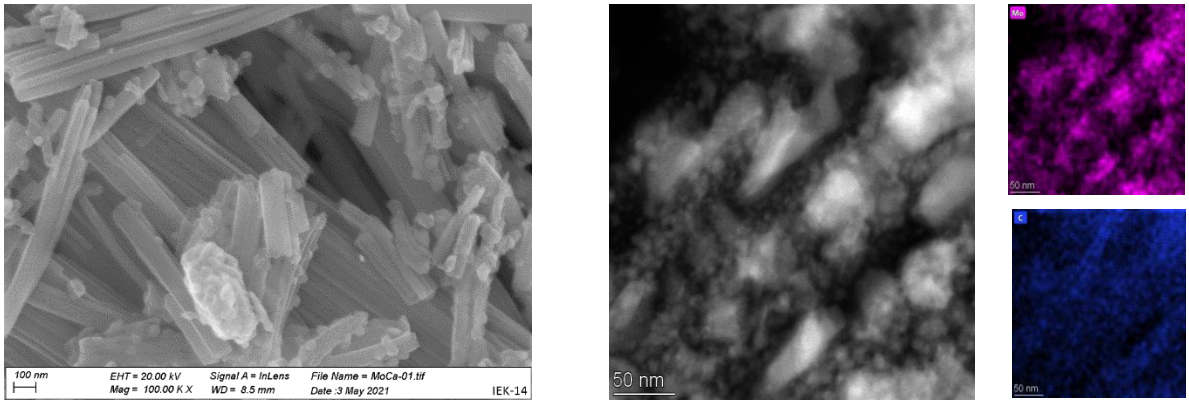

(a) (b)

Figure 11. (a) SEM and (b) HAADF image with elemental mapping of Mo_2C

As we can see in SEM image (figure 11a) that synthesized Mo_2C has a nanowire morphology as intended. However, these nanowires are bundled together. In HAADF (figure 11b) image we can see that these nanowires are not ca single crystalline but are made up of small crystallites and have nanopores in between them.

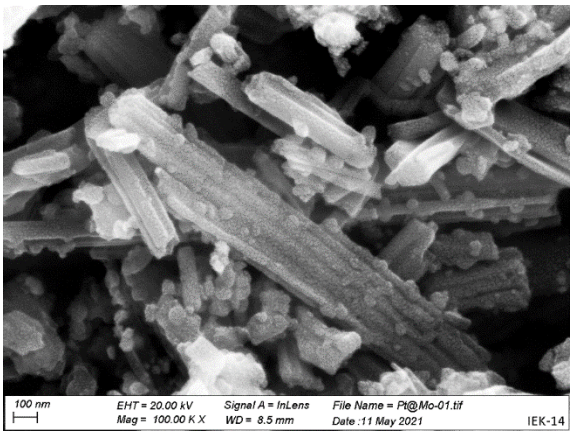

(a)

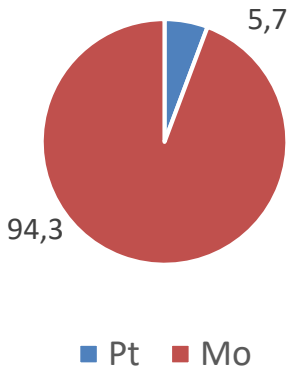

(b)

Figure 12. (a) SEM image and (b) elemental composition of Pt@Mo_2C (5 Wt.%)

In figure 12 (a) we can see that Pt has been deposited on the Mo_2C. It is also notable that the Mo_2C nanowire morphology was not disturbed during the Pt deposition synthesis. With EDX (figure 12b) we determined that the Pt loading on Mo_2C was 5.7 %, a little more than intended.

To understand the dispersion of Pt on Mo_2C, TEM of the developed catalyst was dome. As we can see in the figure 13a that the Pt nanoparticles are not homogeneously dispersed but are severely agglomerated. BET surface area of the developed catalyst also 15% that of the available commercial Pt@C (20 Wt.%), which shows that the active area for catalysis is significantly less than that or Pt@C (fig. 13b).

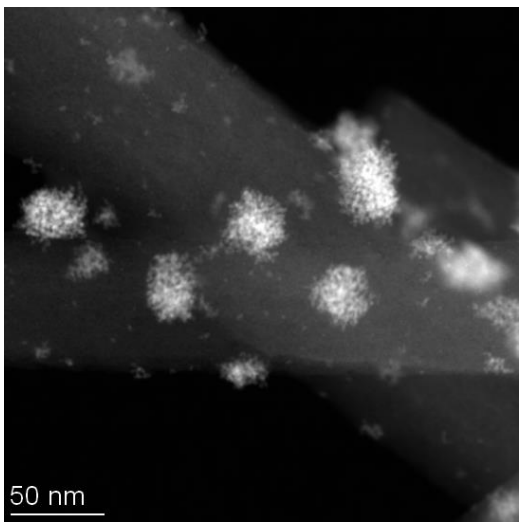

(a)

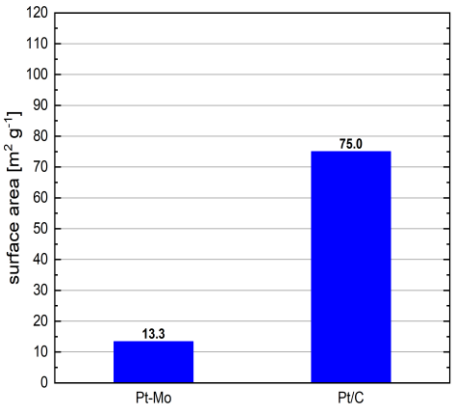

(b)

Figure 13. (a)HAADF image and (b) BET surface of Pt@Mo_2C (5 Wt.%)

2.3.2 Electrochemical characterization

Electrochemical measurements (cyclic voltammetry (CV) and linear polarization were performed in a three-electrode electrochemical cell. All the experimental details, equipment and environment remain the same as our OER catalyst except the ionomer to catalyst ratio 0.33 and loading of catalyst was 80 and 10 µg cm^{-2} for Pt@C (40 wt.%) and Pt@ Mo_2C (5 wt.%). HER activity was evaluated by performing linear sweep voltammetry between 0.01V and -0.2V.

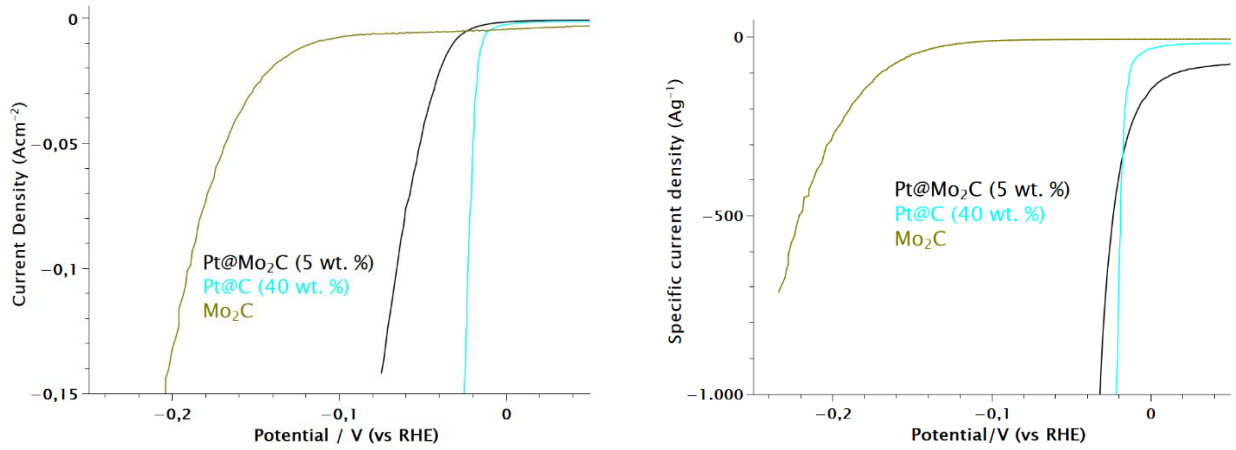

(a) (b)

Figure 14. (a) Area specific and (b) mass specific OER activity comparison on commercial Pt@C (40 wt.%), used support Mo_2C and newly developed Pt@Mo_2C (5 wt.%) catalyst

Figure 14(a) and 14(b) shows area (geometric) and mass normalised LSV curve for the HER catalysts. As can be seen in figure 14(a) area specific current density newly developed Pt@ Mo_2C (5 wt.%) has been found to have comparable HER activity to commercial Pt@C (40 wt.%) at 10mA cm^{-2}. The mass specific HER activity as shown in figure 14(b) of the synthesized Pt@ Mo_2C (5 wt.%) was found to be better than that of commercial Pt@C (40 wt.%) and lower mass normalised current densities, however, lag the commercial Pt@C (40 wt.%) at higher current densities. These results show that the amount of noble metal can be reduced without affecting the HER activity in RDE measurements. Long term testing is going on at CENmat to analyze the stability of as synthesized catalyst.

3g of Pt@ Mo_2C (5 wt.%) and 1.5g Mo_2C of catalyst was sent to FZJ in Mar'21 for testing the catalyst in a single cell.

Single cell testing is performed by FZJ (figure15). For Mo_2C the polarization curve could not be obtained. The exact reason is not very clear, but the interaction of material with the membrane may be a possible reason.

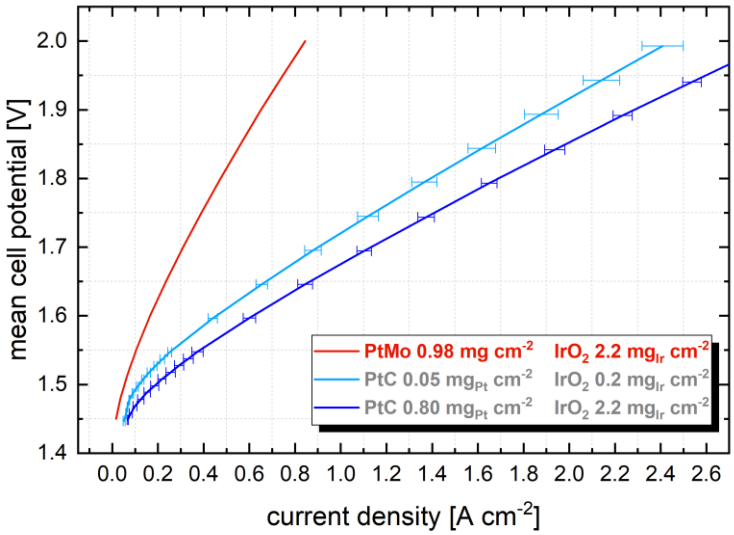

Figure 15. Polarization curve of Pt@Mo_2C (5 Wt.%), and Pt@C

As we can see that the commercial Pt@C has much better performance than the newly developed catalyst. The deficient performance could be attributed to inhomogeneous dispersion of Pt on Mo_2C and the reduced surface area of the Pt@Mo_2C. New synthesis routes are being discovered to disperse the Pt in a homogeneous way on Mo_2C. CENmat is preparing Pt/C (40 wt.%) for further purposes and testing.

On the front of upscaling, Mo_2C can be synthesized in 12g batches and Pt@Mo_2C catalyst can be synthesized in batches of 5g.

3 CRM free Catalysts

3.1 Oxygen Evolution Reaction (OER)

Partner *CNR (Consiglio Nazionale delle Ricerche)* is working on the CRM free catalyst. $Ag_{metallic}$ dispersed on Ti-suboxides catalyst was synthesized by a solid-state procedure starting from $AgNO_3$ (Carlo Erba) precursor and a titanium suboxides (Ti_nO_{2n-1}) powder.

3.1.1 Synthesis and Physicochemical Characterization

Titanium suboxides (Ti_nO_{2n-1}) ceramic powders were prepared from a commercial titanium (IV) chloride solution ($TiCl_4$, Aldrich) by complexation of Ti ions and successive decomposition of the complex to form an amorphous oxide. A high temperature reduction (1050°C) of the amorphous oxide was carried out by using diluted hydrogen. The reagents ($AgNO_3$ and titanium suboxides) were mechanically mixed in the molar ratio of 1:2.3 in a porcelain mortar and were ball milled in a planetary mill for 12 h/300 rpm in order to obtain Ag/Ti-suboxide (Fig. 16a). This Ag/Ti-suboxide was subjected to a thermal treatment (300°C/1h with 50% H_2/Ar) in order to improve the stability of silver by alloying it with the Ti-suboxides (Fig. 16b).

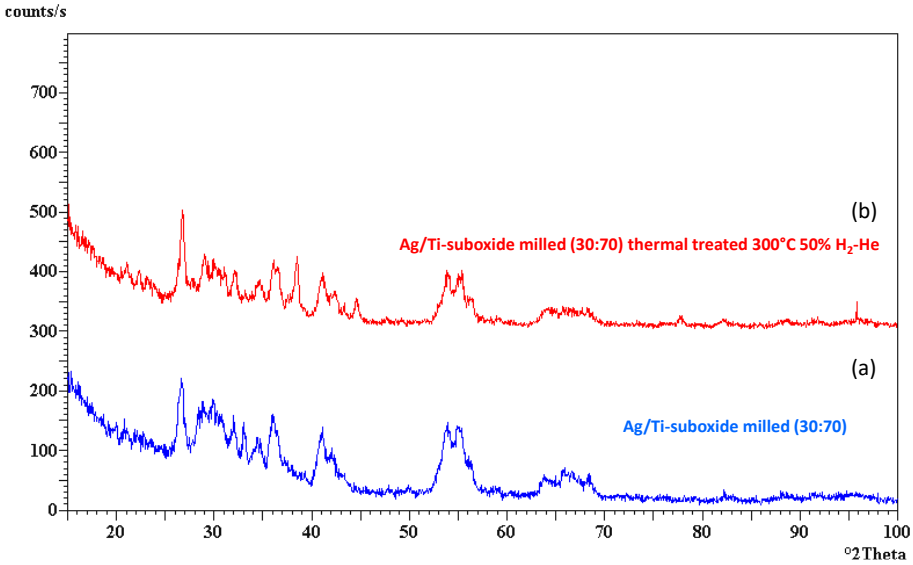

Figure 16. X-ray diffraction patterns of Ag/Ti-suboxide (a), Ag/Ti-suboxide after thermal treated (b)

3.1.2 Electrochemical characterization: *Half cell*

A preliminary screening was carried out with the nonprecious anode electrocatalyst in half cell. Composition and characteristic of the non CRM (according to 2017 EU classification) anode electrocatalyst tested in half cell are reported in Table 1.

Sample	Ball milling Zirconia grinding bowl	Catalyst loading/ mg/cm² (Ti mesh Electrode)	BET m²/g	mA cm⁻²@1.8V vs. RHE (IR-free)	V vs. RHE (Ir-free)	Overpotential mV vs. RHE (Ir-free)	Rs / Ω·cm²
Ag/TiSuboxides (1:2.3) milled	*12 h/300 RPM*	0.5	5.7	4.2	1.97 @9.5mAcm⁻²	490 mV @9.5mAcm⁻²	2.5

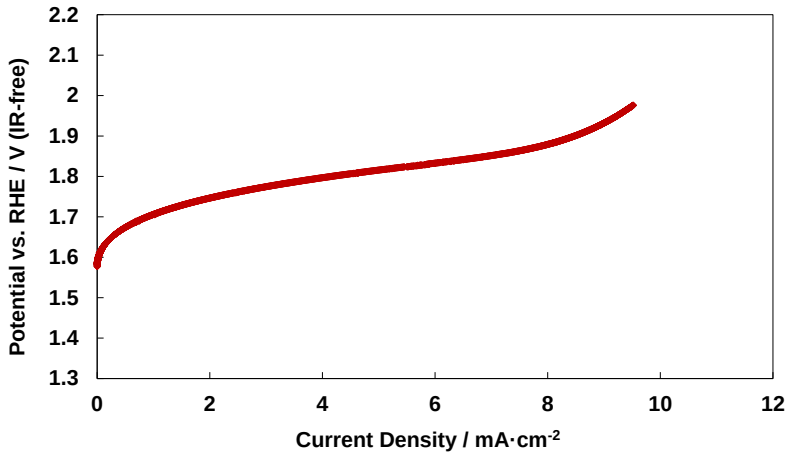

Figure 17. OER activity in acidic electrolyte of Ag/Ti-suboxide electrocatalyst

3.1.3 Electrochemical characterization: *Single cell*

3.1.3.1 Preparation of the membrane-electrode assembly (MEA)

A slurry composed of 80 wt.% catalyst and 20 wt. % Nafion ionomer (5 wt.% Ion Power solution) in deionised water and anhydrous absolute ethanol alcohol (Carlo Erba) was prepared by mixing under ultrasounds. The slurry was directly deposited by using a spray coating technique onto a Titanium fiber mesh, 300 µm thick, characterized by about 70 % porosity. A benchmark 30% Pt/Vulcan catalysts was used as the catalyst for the H_2 evolution. The cathode catalyst was spread onto carbon cloth backing (GDL HT carbon, 300 µm thick carbon cloth) with a Pt loading of 0.5 mg·cm^{-2}. The ionomer content in the cathode layer was 33 wt. % after drying. A Nafion 212 membrane was used for the test in single cell. The MEA, with 5 cm^2 geometrical area, was prepared by a hot-pressing procedure by lamination at 130 °C for 2 min.
Composition and characteristic of the non CRM (according to 2017 EU classification) anode electrocatalyst tested in single cell are reported in Table 2

Anode Catalyst	Anode Catalyst loading/ mg/cm² (Pt-Ti mesh Electrode)	Membrane	Cathode Catalyst	Cathode Catalyst loading/ mg/cm² (GDL Electrode)	V@0.6 A cm⁻² (IR-free) (Single cell Target 0.6 - 1 Acm⁻² @ 1.8V vs.IR free)	Degradation Rate
Ag/Ti-suboxide milled (30:70) -300°C/H_2-He	12.0 (20% NAFION)	212	30% Pt/C	0.5 (33% Nafion)	2.00	< 0.3 % in 1000 h test @ 0.6 A·cm⁻²

3.1.3.2 Electrochemical characterization

The 5 cm^2 PEM single cell electrolyser performance was evaluated at 80 °C and under atmospheric pressure. Deionised water was pre-heated at the same cell temperature and supplied by a pump, at a flow rate of 4 $ml \cdot min^{-1}$, to the anode compartment. Polarization curves (cell potential as a function of current density) and electrochemical impedance spectroscopy (EIS) were carried out by a PGSTAT Autolab 302 Potentiostat/Galvanostat equipped with a booster of 20 A (Metrohm) and a Frequency Response Analyser (FRA). The EIS measurements were performed under potentiostatic control in a frequency range between 20 kHz and 0.1 Hz by frequency sweeping in the single sine mode. The amplitude of the sinusoidal excitation signal was 0.01 V r.m.s. The series resistance was determined from the high frequency intercept on the real axis in the Nyquist plot.

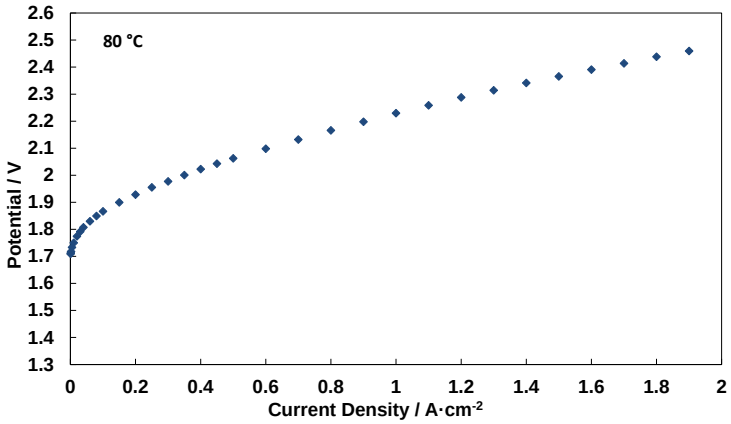

Figure 18. Polarization curve for selected non CRM (according to 2017 EU classification) anode electrocatalysts based MEA

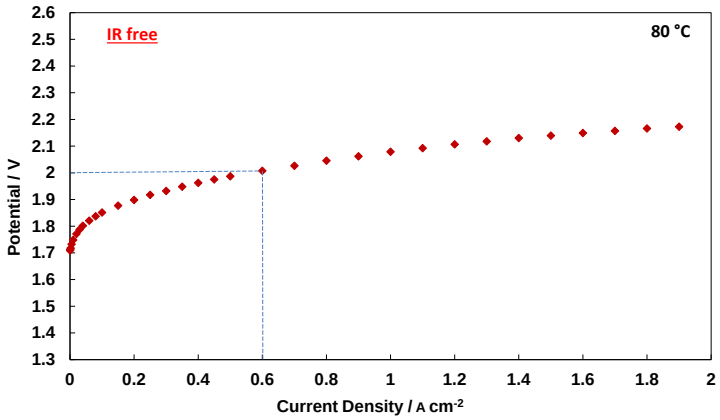

Figure 19. IR-free Polarization curve for selected non CRM anode electrocatalyst based MEA

The Ag/Ti-suboxide catalyst milled (30-70) thermal reduced at in H_2-He showed IR-free single cell performance 200 mV far from the project target (2 V vs. 1.8 V at 0.6 A·cm^{-2}). In order to improve the catalytic activity of the thermal treated of the Ag/Ti-suboxide catalyst milled (30-70), strategies of optimization and investigation will be planned, as for example increase the amount of H_2 flow during the heat treatment.

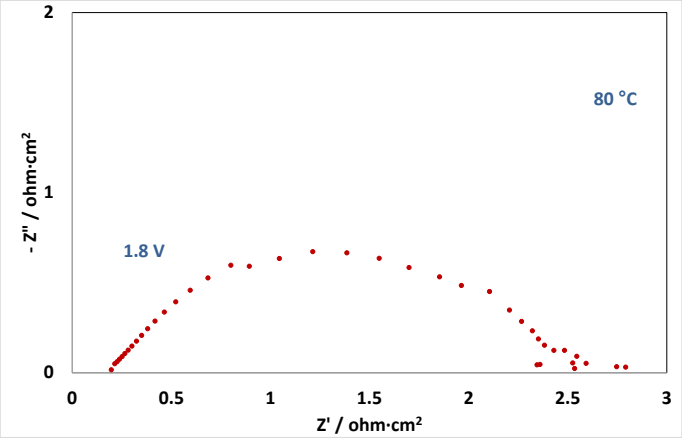

Figure 20.8 EIS for selected non CRM (according to 2017 EU classification) anode electrocatalyst based MEA at 1.8 V and 80°C

Long term stability (1000 h) was appropriate for the Ag/Ti-suboxide electrocatalyst; however, cell voltage is much higher compared to conventional CRM anode based MEAs despite the significantly larger catalyst loadings. For the Ag/Ti-suboxide (30:70) thermal reduced in H_2-He with 20% of ionomer based MEA the voltage efficiency increase by time with a a degradation rate of 10 µV/h by removing the first 10 h conditioning period, that correspond to < *0.3 % in 1000 h* (*project target: < 1% in 1000 h for the anode CRM free catalyst*).

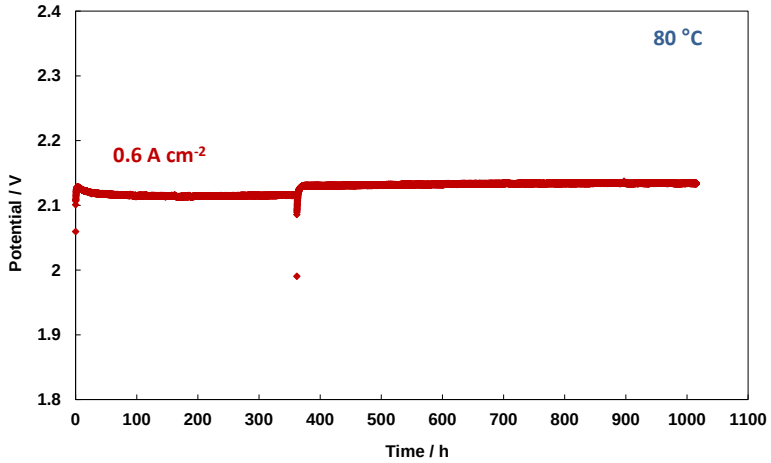

Figure 21. Chrono-potentiometric test at 0.6 A·cm^{-2} and 80 °C for selected non CRM (according to 2017 EU classification) anode electrocatalyst based MEA

3.2 Hydrogen Evolution Reaction (HER)

CSIC has prepared MoS_2 dispersed onto an active carbon (Black Pearls), as CRM-free electrocatalyst for the hydrogen evolution reaction.

3.2.1 Synthesis and Physicochemical Characterization

MoS_2 dispersed on black pearls (MoS_2/BP) was prepared through a solvothermal synthesis route with rather easy scalability. CSIC has started with the synthesis of MoS_2 supported on different carbon structures.

The characterization of MoS_2/BP has been performed. First of all, x-ray diffraction was used to determine the crystal structure of the sulphide. The crystallinity of the sulphide is too low to allow a proper structural study (Figure 22a, left). TEM was also performed to analyze composition and morphology. An atomic ratio of Mo:S 1:2 was determined, in good agreement with the composition expected for MoS_2. The morphology of the catalyst is a very disordered layered material (Figure 22a, right).

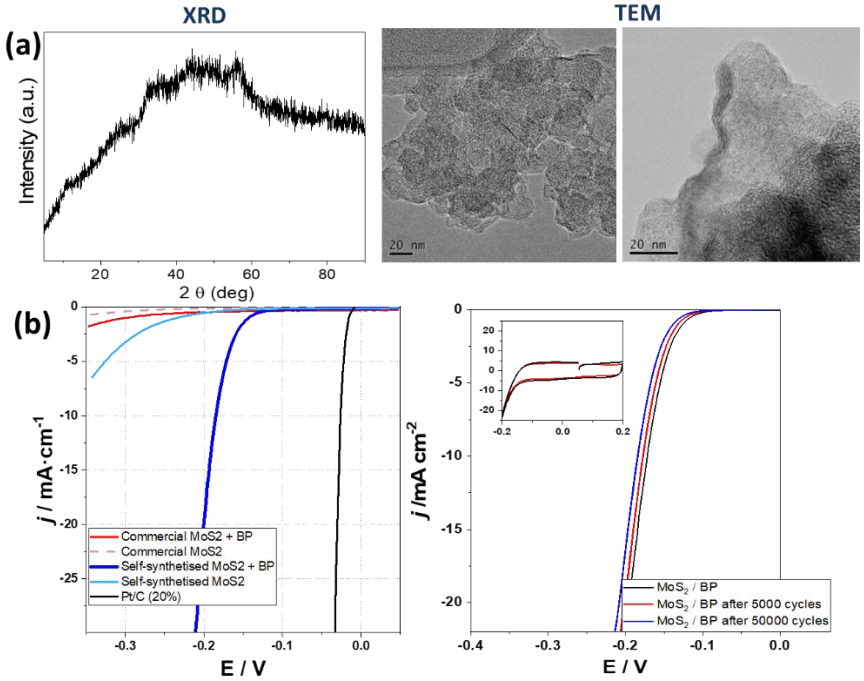

Figure 22. (a) Physicochemical Characterization of MoS_2/BP. (b) Electrochemical Characterization for the HER using MoS_2/BP

3.2.2 Electrochemical Performance

OER Activity

Catalyst conditioning was performed in Ar-saturated electrolytes by recording cyclic voltammograms at scan rate 50 mV/s between 0.05 and 0.45 V (*vs*. RHE) in 0.5 M H_2SO_4. For the HER measurements the electrolyte is saturated with H_2 and cyclic voltammograms are recorded at 5 mV/s and 1600 rpm in a window potential between -0.05 and -0.4 V.

The HER measurements have been performed with MoS_2 synthetized at *CSIC* and commercial MoS_2 both with and without BP. The HER activities were compared with 20%Pt/C. Figure 22b, left, shows the HER activities. The addition of BP shows an improvement of the catalytic activity of both *CSIC*'s and commercial MoS_2. The HER activity of the MoS_2 synthesized at *CSIC* has a much better performance. This can be explained by considering that *CSIC*'s MoS_2 is less crystalline and probably exposing a higher fraction of active sites. In fact, the activity of *CSIC*'s MoS_2/BP (overpotential of 148 mV *vs.* RHE at 10 mA/cm^2) is one of the best HER activities reported so far for a molybdenum sulphide catalysts [14–16].

OER Durability

Durability of MoS_2/BP was tested in an RDE configuration by recording 50000 consecutive cycles between -0.2 V and 0.2 V (inset Figure 5b, right). As it can be seen in Figure 5b right, the activity of MoS_2/BP remains stable after 50000 cycles under such conditions.

3.2.3 PEM Electrolyzer testing

2g of MoS_2/BP were sent to Forschungszentrum Jülich (FZJ) on October 2020 to be tested on single cell electrolyzer. The MEAs have being tested at different loadings. MoS_2/BP MEAs results tested by FZJ are included in the Deliverable D1.2.

Non-PGM materials provide a cost-effective alternative to replace PGM catalysts. MoS_2 was used as the HER catalysts to replace Pt in the cathode side. The ink made from MoS_2 contains n-propanol and water at less than 0.5% by weight, as this is most effective for stabilization, and was then sonicated in ice bath for at least 30 minutes. The MoS_2/BP ink was sprayed directly onto the Nafion N117 membrane to verify the required loading and performance of this PGM-free catalyst. Figure 23 shows that the performance of MEA with MoS_2/BP (anode: 2.2 mg_{Ir} cm^{-2}) cannot compete with the performance of MEA with low PGM loading (0.2 mg_{Ir} cm^{-2} & 0.05 mg_{Pt} cm^{-2}) and also increasing the loading of MoS_2 resulted in the same performance.

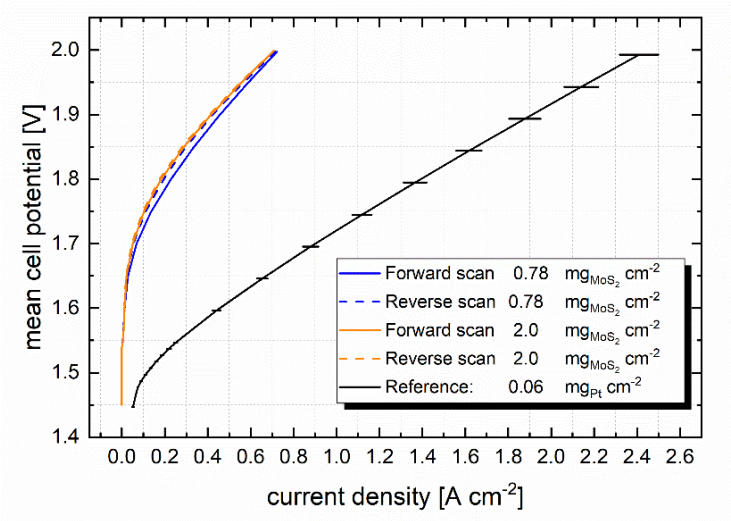

Figure 23. Performance screening for the MoS_2/BP catalyst with two different loadings on a Nafion N117 membrane

Comparison of our results (Figure 24a) with the literature (Figure 24b) shows similar performance. The performance from our study showed a current density of 0.17 A cm^{-2} at 1.8 V while the MEA

presented by Corrales-Sánchez et al.[17] in 2014, obtained a current density of 0.18 A cm^{-2} at 1.8V. They obtained a constant current density of ca. 0.35 A cm^{-2} at 2V, after a continuous operation of 15 h. Our study obtained a current density of 0.71 A cm^{-2} after 10 polarization curves (forward & reverse).

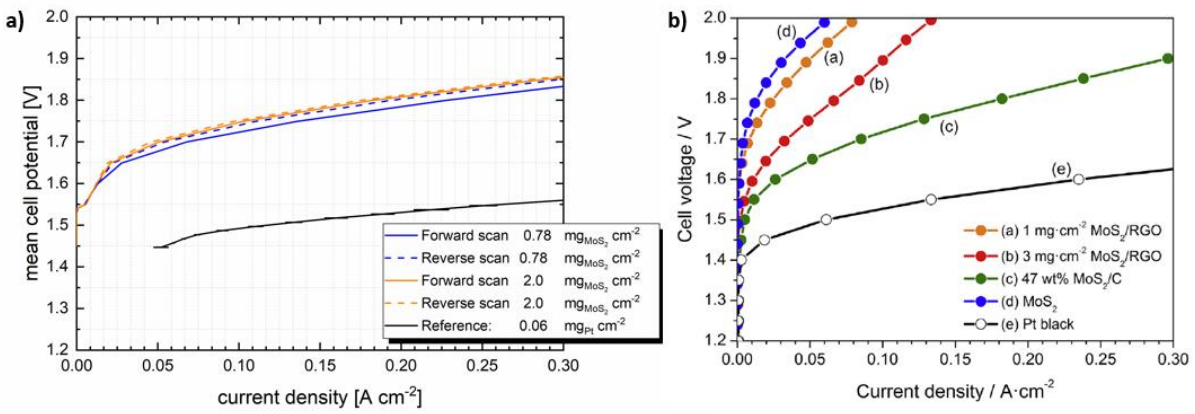

Figure 24. Comparison of the results of this study with results from Corrales-Sánchez et *al.*[17] indicating a similar trend of performance

4 Comparison of developed catalysts

One of overall goals of this project is the development and production of advanced catalysts based on reduced PGM loading and CRM-free anodes and cathodes to replace or drastically reduce the critical raw materials content of anode and cathode catalyst layers in PEMWE while maintaining good performance and durability. A comparison of developed catalysts to date is reported in the following.
Composition and characteristics of the anode and cathode electrocatalysts tested in single cell are reported in Table 3.

Table 3. Anode and cathode electrocatalysts assessed in single cell. The formulations developed in the project are highlighted in bold.

Anode Catalyst	Anode Catalyst loading/ mg/cm² (Pt-Ti mesh Electrode)	Membrane	Cathode Catalyst	Cathode Catalyst loading/ mg/cm² (GDL Electrode)
Ag/Ti-suboxide (30:70)	12.0 (20% NAFION)	N212	30% Pt/C	0.5 (33% Nafion)
IrO_2	2.2 (25% NAFION)	N117	**MoS_2**	0.8 (25% Nafion)
Ir-ATO 50wt.%	0.2 (20% NAFION)	N117	60% Pt/C	0.8 (20% Nafion)

Partner *CSIC and CENmat* are working on several catalysts for the HER with low content of CRMs. However, no candidates have been yet selected to be assessed in MEAs.

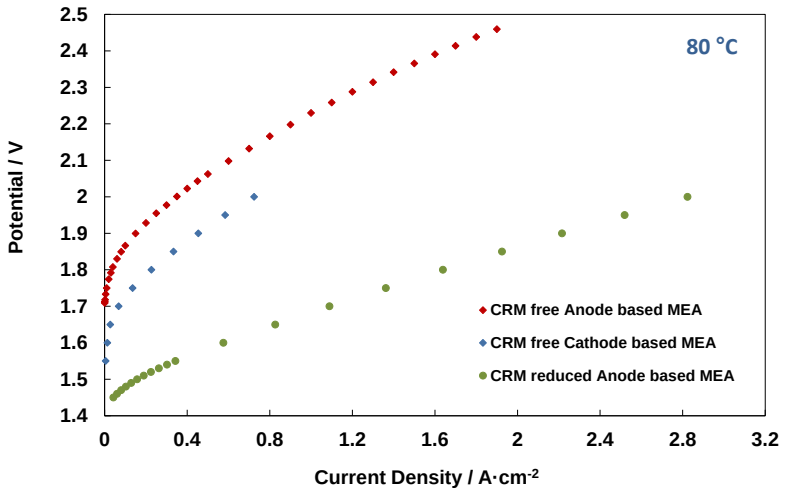

Figure 25. Polarization curves for MEAs based on selected electrocatalysts

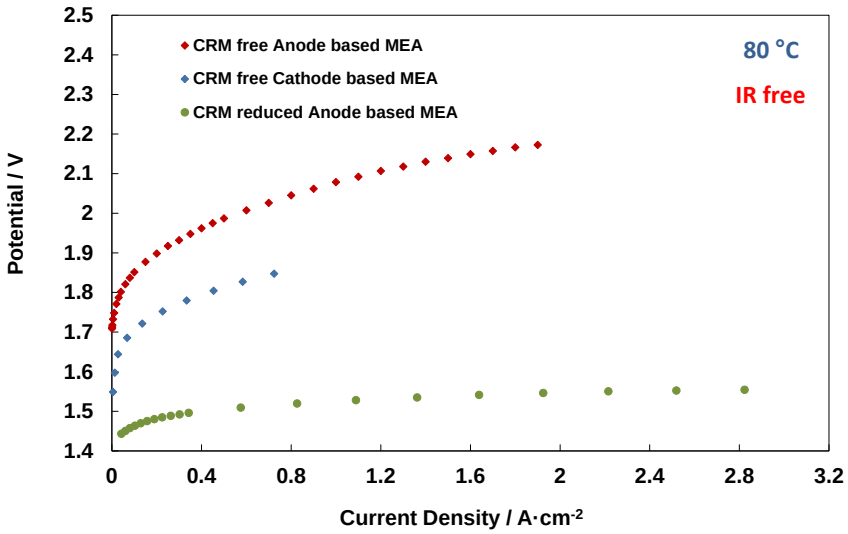

Figure 26. IR-free Polarization curves for MEAs based on selected electrocatalysts

IR-free single cell performance of CRM free anode based MEA (red points) resulted 200 mV far from the project target (2 V vs. 1.8 V at 0.6 A·cm^{-2}). In order to improve the catalytic activity of the CRM free anode catalyst, strategies of optimization and investigation are planned, as for example modification of the thermal treatment etc. Regarding the IR-free single cell performance of reduced CRM anode based MEA (green points), it was recorded 2.83 A·cm^{-2} at 1.55 V (project target: > 2 A·cm^{-2} at 1.8 V).

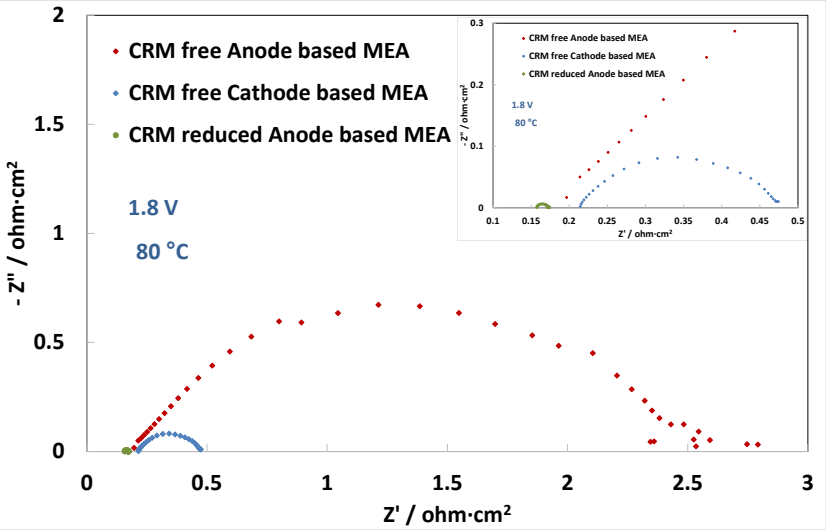

Figure 27.9 EIS at 1.8 V and 80°C for MEAs based on selected electrocatalysts

Impedance results show the very low polarisation resistance of the reduced CRM anode electrocatalyst based MEA. Whereas polarisation resistance is very large for the CRM materials; the series resistance is very similar indicating that the membrane contribution is similar in all these experiments.

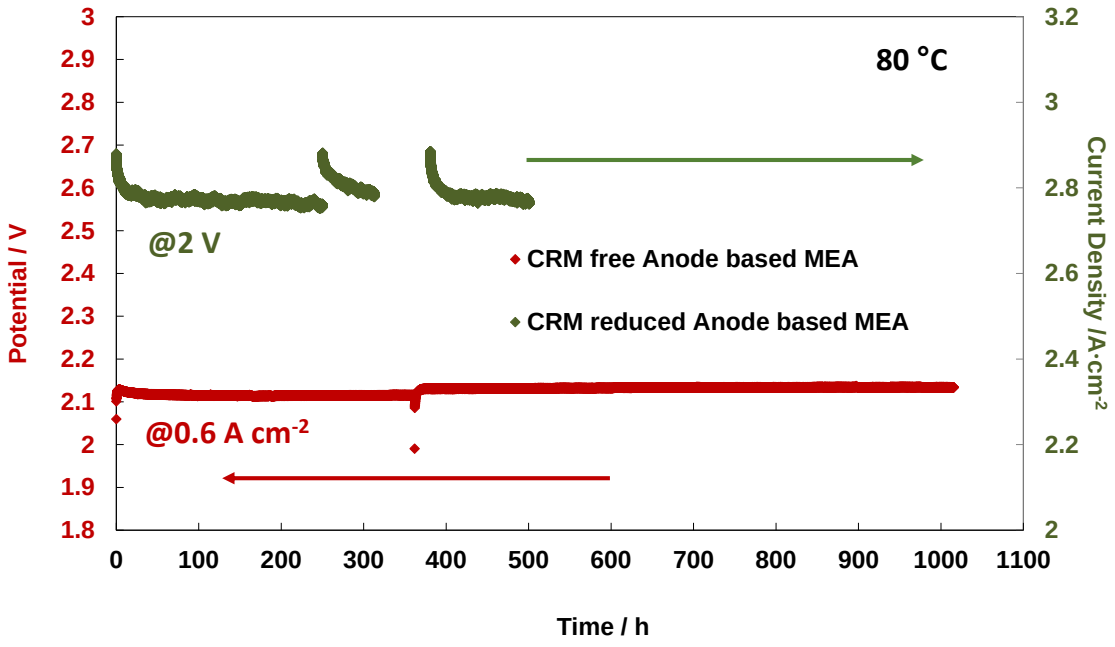

Figure 28. Chrono-potentiometric test at 0.6 A·cm^{-2} and 80 °C for MEA based on selected non CRM (according to 2017 EU classification) anode electrocatalyst (red curve) and

chrono-galvanometric test at 2 V and 80 °C for selected MEA based on reduced CRM anode electrocatalyst (green curve)

Long term stability (1000 h) was appropriate for the CRM free Anode based MEA; however, cell voltage is much higher compared to conventional CRM anode based MEAs despite the significantly larger catalyst loadings. The voltage efficiency increases by time with a degradation rate of 10 µV/h by removing the first 10 h conditioning period, that correspond to *< 0.3 % in 1000 h* (*project target: < 1% in 1000 h for the anode CRM free catalyst*). Whereas for the long term stability (500 h) test on the CRM reduced Anode based MEA, the current density decreases by time with a degradation rate of 57 $\mu A \cdot cm^{-2}$/h by removing the first 10 h conditioning period.

In conclusion single cell tests based on the developed catalysts have indicated that the performance of non-CRM (according to 2017 EU classification) anode catalyst was significantly lower than the benchmark IrOx catalyst despite the much larger catalyst loading (12 vs conventional 2-3 $mg \cdot cm^{-2}$).
Despite the much lower voltage efficiency of non-CRM catalysts (according to 2017 EU classification) vs. conventional CRM anode catalysts, a relatively good stability was observed.
Significant improvements are needed for non-CRM (according to 2017 EU classification) anode catalysts before these can become competitive with respect to reduced CRM loading anode electrocatalysts.
Regarding the stability, the CRM free anode showed a lower degradation rate compared to the reduced CRM anode based MEA but this could be just related to the different operating current density. It is well know that increasing the operating turnover frequency (higher current density and lower active phase catalyst loading), there is a corresponding increase of the degradation rate [18].
Considering the relevant difference in voltage efficiency, the reduced PGM content anode catalyst is selected for the final stack testing. This will be combined to a conventional PGM cathode containing moderate Pt loading (0.1 mg cm^{-2}) and PFSA membrane.

[1] H.N. Nong, L. Gan, E. Willinger, D. Teschner, P. Strasser, IrOx core-shell nanocatalysts for cost- and energy-efficient electrochemical water splitting, Chem. Sci. 5 (2014) 2955–2963. https://doi.org/10.1039/c4sc01065e.
[2] J. Kim, P.C. Shih, K.C. Tsao, Y.T. Pan, X. Yin, C.J. Sun, H. Yang, High-Performance Pyrochlore-Type Yttrium Ruthenate Electrocatalyst for Oxygen Evolution Reaction in Acidic Media, J. Am. Chem. Soc. 139 (2017) 12076–12083. https://doi.org/10.1021/jacs.7b06808.
[3] T. Schuler, J.M. Ciccone, B. Krentscher, F. Marone, C. Peter, T.J. Schmidt, F.N. Büchi, Hierarchically Structured Porous Transport Layers for Polymer Electrolyte Water Electrolysis, Adv. Energy Mater. 10 (2020) 1903216. https://doi.org/10.1002/aenm.201903216.
[4] F. Scheepers, M. Stähler, A. Stähler, E. Rauls, M. Müller, M. Carmo, W. Lehnert, Improving the Efficiency of PEM Electrolyzers through Membrane-Specific Pressure Optimization, Energies. 13 (2020) 612. https://doi.org/10.3390/en13030612.
[5] S. Siracusano, C. Oldani, M.A. Navarra, S. Tonella, L. Mazzapioda, N. Briguglio, A.S. Aricò, Chemically stabilised extruded and recast short side chain Aquivion® proton exchange membranes for high current density operation in water electrolysis, J. Memb. Sci. 578 (2019) 136–148. https://doi.org/10.1016/j.memsci.2019.02.021.
[6] M. Bernt, J. Schröter, M. Möckl, H.A. Gasteiger, Analysis of Gas Permeation Phenomena in a PEM Water Electrolyzer Operated at High Pressure and High Current Density, J. Electrochem. Soc. 167

(2020) 124502. https://doi.org/10.1149/1945-7111/abaa68.
[7] F.J. Hackemüller, E. Borgardt, O. Panchenko, M. Müller, M. Bram, Manufacturing of Large-Scale Titanium-Based Porous Transport Layers for Polymer Electrolyte Membrane Electrolysis by Tape Casting, Adv. Eng. Mater. 21 (2019) 1801201. https://doi.org/https://doi.org/10.1002/adem.201801201.
[8] K.E. Ayers, J.N. Renner, N. Danilovic, J.X. Wang, Y. Zhang, R. Maric, H. Yu, Pathways to ultra-low platinum group metal catalyst loading in proton exchange membrane electrolyzers, Catal. Today. 262 (2016) 121–132. https://doi.org/https://doi.org/10.1016/j.cattod.2015.10.019.
[9] P. Lettenmeier, R. Wang, R. Abouatallah, S. Helmly, T. Morawietz, R. Hiesgen, S. Kolb, F. Burggraf, J. Kallo, A.S. Gago, K.A. Friedrich, Durable Membrane Electrode Assemblies for Proton Exchange Membrane Electrolyzer Systems Operating at High Current Densities, Electrochim. Acta. 210 (2016) 502–511. https://doi.org/10.1016/j.electacta.2016.04.164.
[10] P. Lettenmeier, S. Kolb, N. Sata, A. Fallisch, L. Zielke, S. Thiele, A.S. Gago, K.A. Friedrich, Comprehensive investigation of novel pore-graded gas diffusion layers for high-performance and cost-effective proton exchange membrane electrolyzers, Energy Environ. Sci. 10 (2017) 2521–2533. https://doi.org/10.1039/c7ee01240c.
[11] S. Siracusano, S. Trocino, N. Briguglio, V. Baglio, A.S. Aricò, Electrochemical Impedance Spectroscopy as a Diagnostic Tool in Polymer Electrolyte Membrane Electrolysis, Mater. . 11 (2018). https://doi.org/10.3390/ma11081368.
[12] C. Rozain, E. Mayousse, N. Guillet, P. Millet, Influence of iridium oxide loadings on the performance of PEM water electrolysis cells: Part II – Advanced oxygen electrodes, Appl. Catal. B Environ. 182 (2016) 123–131. https://doi.org/https://doi.org/10.1016/j.apcatb.2015.09.011.
[13] M. Eikerling, A.A. Kornyshev, Electrochemical impedance of the cathode catalyst layer in polymer electrolyte fuel cells, J. Electroanal. Chem. 475 (1999) 107–123. https://doi.org/https://doi.org/10.1016/S0022-0728(99)00335-6.
[14] T.F. Jaramillo, K.P. Jørgensen, J. Bonde, J.H. Nielsen, S. Horch, I. Chorkendorff, Identification of active edge sites for electrochemical H2 evolution from MoS2 nanocatalysts, Science (80-.). 317 (2007) 100–102. https://doi.org/10.1126/science.1141483.
[15] Y. Yan, B. Xia, Z. Xu, X. Wang, Recent development of molybdenum sulfides as advanced electrocatalysts for hydrogen evolution reaction, ACS Catal. 4 (2014) 1693–1705. https://doi.org/10.1021/cs500070x.
[16] B. Hinnemann, P.G. Moses, J. Bonde, K.P. Jørgensen, J.H. Nielsen, S. Horch, I. Chorkendorff, J.K. Nørskov, Biomimetic Hydrogen Evolution: MoS 2 Nanoparticles as Catalyst for Hydrogen Evolution, J. Am. Chem. Soc. 127 (2005) 5308–5309. https://doi.org/10.1021/ja0504690.
[17] T. Corrales-Sánchez, J. Ampurdanés, A. Urakawa, MoS2-based materials as alternative cathode catalyst for PEM electrolysis, Int. J. Hydrogen Energy. 39 (2014) 20837–20843. https://doi.org/10.1016/j.ijhydene.2014.08.078.
[18] Stefania Siracusano, Nejc Hodnik, Primoz Jovanovic, Francisco Ruiz-Zepeda, Martin Šala, Vincenzo Baglio, Antonino Salvatore Aricò. New insights into the stability of a high performance nanostructured catalyst for sustainable water electrolysis. Nano Energy 40 (2017) 618-632

Acknowledgement

This project has received funding from the European Union's Horizon 2020 research and innovation programme under grant agreement No 862253".